

Electronic Supplementary Information

For

**Trifunctional Ir^{III}ppy-type asymmetric phosphorescent emitters
with ambipolar features for highly efficient electroluminescent
devices**

Xianbin Xu, Xiaolong Yang, Jingshuang Dang, Guijiang Zhou,* Yong Wu,* and Wai-Yeung Wong*

Experimental

General information: All reactions were performed under an inert nitrogen atmosphere. All the solvents were carefully dried and distilled from appropriate drying agents prior to use. All the commercially available chemicals were used directly with no further purification. All reactions were monitored by thin-layer chromatography (TLC) with Merck pre-coated aluminium plates. Flash column chromatography and preparative TLC were carried out using silica gel from Shanghai Qingdao (200-300 mesh). ^1H NMR and ^{13}C NMR spectra were measured in CDCl_3 on a Bruker Advance 400 MHz spectrometer and chemical shifts were quoted relative to the solvent residual peak at δ 7.26 for ^1H and 77.0 for ^{13}C nuclei, respectively.

Physical measurements: The thermal gravimetric analysis (TGA) was performed on a NETZSCH STA 409C instrument under a nitrogen atmosphere at the heating rate of 20 K min^{-1} . Differential scanning calorimetry (DSC) was conducted on a NETZSCH DSC 200 PC unit under a nitrogen flow at a heating rate of 10 K min^{-1} . UV-vis spectra were recorded at room temperature on a Shimadzu UV-2250 spectrophotometer. Emission spectra and lifetimes of the complexes were measured using an Edinburgh Instruments Ltd (FLSP920) fluorescence spectrophotometer. The data analysis was conducted by iterative convolution of the luminescence decay profile with the instrument response function using the software package provided by Edinburgh Instruments. The phosphorescence quantum yields (Φ_{P}) were determined in CH_2Cl_2 solutions at 298 K against *fac*-[Ir(ppy)₃] standard ($\Phi_{\text{P}} = 0.40$).^{S1} The mass spectra were obtained on micrOTOF-Q II 10280 with very mild ESI ion source to avoid the decomposition of the complex molecules as far as possible. Electrochemical measurements were made using a Princeton Applied Research model 273A potentiostat. The cyclic voltammetry experiment of the sample solution was performed at a scan rate of 100 mV

s^{-1} using a glassy carbon working electrode, a platinum counter electrode and a platinum-wire reference electrode. The solvent in all measurements was deoxygenated acetonitrile, and the supporting electrolyte was 0.1 M [$^n\text{Bu}_4\text{N}$][PF_6^-]. Ferrocene was added as a calibrant after each set of measurements, and all potentials reported were quoted with reference to the ferrocene-ferrocenium (Fc/Fc^+) couple. The oxidation (E_{ox}) and reduction (E_{red}) potentials were used to determine the HOMO and LUMO energy levels using the equations $E_{\text{HOMO}} = -(E_{\text{ox}} + 4.8)$ eV and $E_{\text{LUMO}} = -(E_{\text{red}} + 4.8)$ eV which were calculated using the internal standard ferrocene value of -4.8 eV with respect to the vacuum level.

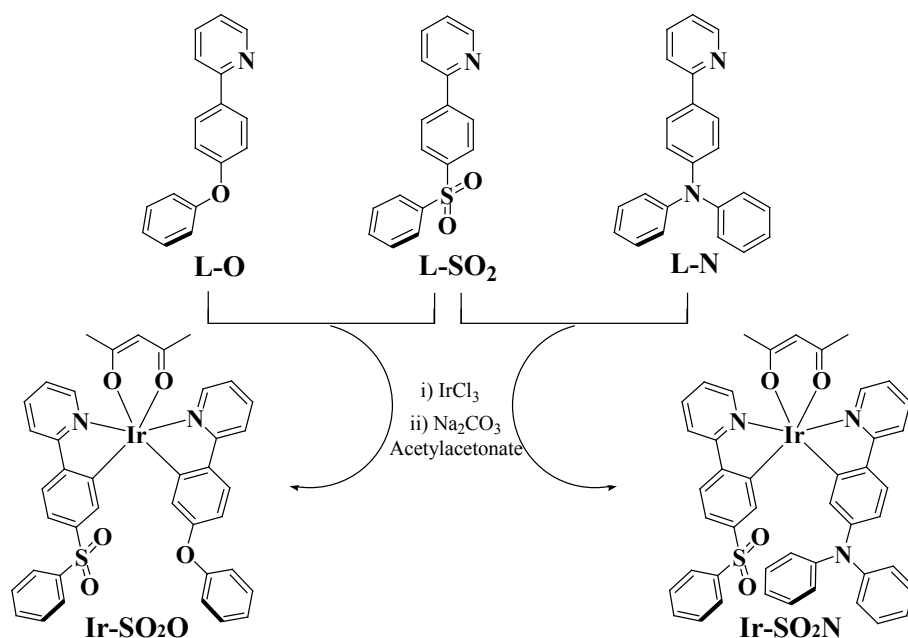


Fig. S1 Synthetic routes for the new asymmetric Ir^{III} complexes **Ir-SO₂O** and **Ir-SO₂N**.

The organic ligands were prepared according to the literature method.^{4a}

The general synthetic procedure for the iridium(III) complexes: Under a N_2 atmosphere, 1.0 equivalent **L-O** or **L-N**, 1.0 equivalent **L-SO₂**, and 0.8 equivalent $\text{IrCl}_3 \cdot n\text{H}_2\text{O}$ were added to a mixture of 2-ethoxyethanol and water (3:1, v/v). The reaction mixture was

heated to 110 °C for 18 h under stirring. After cooling the mixture to room temperature, saturated NaCl solution was added to the reaction mixture. The precipitate formed was collected by filtration and dried under vacuum to give an orange solid. Together with the orange solid, 10.0 equivalent Na₂CO₃ and 5.0 equivalent acetylacetone were added to 2-ethoxyethanol. The reaction mixture was heated to 110 °C for 16 h with stirring. Water was added to the reaction mixture after it was cooled to room temperature. The mixture was extracted with CH₂Cl₂ and the combined organic phase was dried over MgSO₄. The solvent was removed under reduced pressure and the residue was purified on preparative TLC plates with CH₂Cl₂/diethyl ether as the eluent.

Ir-SO₂O: (Eluent: CH₂Cl₂/diethyl ether (35:1, v/v). Yield 20%). ¹H NMR (400 MHz, CDCl₃): δ (ppm) 8.47 (d, *J* = 6.0 Hz, 1H, Ar), 8.38 (d, *J* = 5.6 Hz, 1H, Ar), 7.80–7.75 (m, 3H, Ar), 7.69 (d, *J* = 7.6 Hz, 1H, Ar), 7.65 (d, *J* = 8.0 Hz, 2H, Ar), 7.55 (d, *J* = 8.0 Hz, 1H, Ar), 7.48–7.42 (m, 2H, Ar), 7.37 (d, *J* = 7.6 Hz, 2H, Ar), 7.32 (t, *J* = 8.0 Hz, 1H, Ar), 7.20–7.14 (m, 4H, Ar), 7.00 (t, *J* = 7.2 Hz, 1H, Ar), 6.77 (d, *J* = 8.0 Hz, 2H, Ar), 6.73 (s, 1H, Ar), 6.36 (dd, *J* = 2.0 Hz, 8.4Hz, 1H, Ar), 5.68 (d, *J* = 2.4 Hz, 1H, Ar), 5.24 (s, 1H, acac), 1.82 (s, 3H, Me), 1.77 (s, 3H, Me). ¹³C NMR (100 MHz, CDCl₃): δ (ppm) 184.83, 184.75 (acac), 167.63, 157.56, 156.45, 149.95, 148.65, 148.49, 148.05, 141.94, 139.58, 139.54, 137.34, 137.21, 132.46, 131.12, 129.31, 128.77, 127.42, 125.19, 123.67, 122.99, 121.99, 121.08, 119.78, 119.62, 119.47, 118.27, 110.71 (Ar), 100.58 (acac), 28.70, 28.65 (Me). ESI-TOF (*m/z*): 855 [M+Na]⁺. Anal. calcd. for C₃₉H₃₁IrN₂O₅S: C, 56.30; H, 3.76; N, 3.37; found: C, 56.52; H, 3.48; N, 3.16.

Ir-SO₂N: (Eluent: CH₂Cl₂/diethyl ether (40:1, v/v). Yield 18%). ¹H NMR (400 MHz, CDCl₃): δ (ppm) 8.35 (d, *J* = 7.2 Hz, 2H, Ar), 7.73–7.64 (m, 4H, Ar), 7.59 (d, *J* = 8.0 Hz, 1H, Ar), 7.53–7.44 (m, 3H, Ar), 7.39–7.33 (m, 3H, Ar), 7.29 (s, 1H, Ar), 7.10–7.06 (m, 5H, Ar), 7.00

(t, $J = 2.0$ Hz, 1H, Ar), 6.92 (t, $J = 7.2$ Hz, 2H, Ar), 6.80 (d, $J = 8.0$ Hz, 4H, Ar), 6.76 (s, 1H, Ar), 6.44 (dd, $J = 2.4$ Hz, 8.8 Hz, 1H, Ar), 5.48 (d, $J = 2.0$ Hz, 1H, Ar), 5.24 (s, 1H, acac), 1.83 (s, 3H, Me), 1.78 (s, 3H, Me). ^{13}C NMR (100 MHz, CDCl_3): δ (ppm) 184.74, 184.68, 167.71, 166.31, 149.98, 148.93, 148.25, 147.99, 147.68, 147.20, 146.43, 142.09, 139.35, 137.90, 137.08, 136.67, 132.41, 131.29, 128.94, 128.78, 128.75, 127.34, 125.20, 125.05, 124.72, 124.51, 123.52, 122.85, 122.70, 120.40, 119.58, 119.51, 117.92, 114.56 (Ar), 100.56 (acac), 28.74, 28.71 (Me). ESI-TOF (m/z): 930 [M+Na] $^+$. Anal. calcd. for $\text{C}_{45}\text{H}_{36}\text{IrN}_3\text{O}_4\text{S}$: C, 59.59; H, 4.00; N, 4.63; found: C, 59.37; H, 3.89; N, 4.56.

OLED fabrication and measurements: All the OLEDs were fabricated on the pre-patterned ITO-coated glass substrate having sheet resistance of $30 \Omega \text{ sq}^{-1}$. Substrates were cleaned by ultrasonic bath in detergent before being washed with deionized water and dried at 120 °C for more than 2 h. The ITO substrates were treated by UV ozone for 20 min before being loaded into the vacuum deposition system. Every active layer was formed one by one from the ITO anode to the aluminum cathode according to the pre-designed configuration for the monochromatic OLEDs. The doped emission layer was deposited by co-evaporation from two separate sources. The vacuum pressure was $< 5 \times 10^{-6}$ Torr during deposition of all organic materials and $< 8 \times 10^{-6}$ Torr during the cathode deposition. The J – V – L characteristics of the devices were measured with a computer controlled KEITHLEY 236 source meter and PHOTORESEARCH PR650 spectrophotometer in air without device encapsulation.

Computational details: Geometrical optimizations were conducted using the popular B3LYP functional theory. The basis set used for C, H, N, O and S atoms was 6-311G(d, p) while effective core potentials with a LanL2DZ basis set were employed for Ir atoms.^{S2} The energies of the excited states of the complexes were computed by time-dependent (TD) DFT (TD-DFT)

based on all the ground-state geometries. The various properties of these molecules, such as HOMO, LUMO, ionization potentials (IP), electron affinities (EA) and reorganization energies (λ) were obtained from the computed results. All calculations were carried out using the Gaussian 09 program.^{S3}

X-Ray crystallography: X-Ray diffraction data were collected at 293 K using graphite-monochromated Mo-K α radiation ($\lambda = 0.71073 \text{ \AA}$) on a Bruker Axs SMART 1000 CCD diffractometer. The collected frames were processed with the software SAINT+^{S4} and an absorption correction (SADABS)^{S5} was applied to the collected reflections. The structure was solved by the Direct methods (SHELXTL)^{S6} in conjunction with standard difference Fourier techniques and subsequently refined by full-matrix least-squares analyses on F^2 . Hydrogen atoms were generated in their idealized positions and all non-hydrogen atoms were refined anisotropically. Hydrogen atoms on organic ligands were generated by the riding mode, but not included for the terminal water molecules as they could not be positively identified. The anisotropic displacement parameters of S1 and C25 have been restrained to have an isotropic behavior (ISOR) due to the instability of their anisotropic refinements. For the high atomic temperature factors as compared with the bonded neighbors, the anisotropic displacement parameters of some carbon atoms (C9 and C25) have been restrained to be equal (EADP), respectively. SADI restraints for S1, O2 and O3 were taken to make the two S-O distances approximately equal (with an esd of say 0.01). Some SIMU and DELU restraints of carbon atoms (for C29, C30, C31, C32, C33, C34, C25, C12, C13, C14, C15, C16, C17 and C18) were also performed to restrain their high atomic temperature factors as compared with the bonded neighbors. The crystallographic data for **Ir-SO₂O** (excluding structure factors) have been deposited at the Cambridge Crystallographic Data Centre with the deposition number

CCDC-962561. These data can be obtained free of charge on application to CCDC, 12 Union Road, Cambridge CB2 1EZ, UK (fax: (+44)1223-336-033; E-mail: deposit@ccdc.cam.ac.uk)

References:

- S1. K. A. King, P. J. Spellane and R.-J. Watts, *J. Am. Chem. Soc.*, 1985, **107**, 1431.
- S2. (a) W. R. Wadt and P. J. Hay, *J. Chem. Phys.*, 1985, **82**, 284. (b) P. J. Hay and W. R. Wadt, *J. Chem. Phys.*, 1985, **82**, 299.
- S3. M. J. Frisch, G. W. Trucks, H. B. Schlegel, G. E. Scuseria, M. A. Robb, J. R. Cheeseman, J. A. Montgomery, T. Vreven Jr., K. N. Kudin, J. C. Burant, J. M. Millam, S. S. Iyengar, J. Tomasi, V. Barone, B. Mennucci, M. Cossi, G. Scalmani, N. Rega, G. A. Petersson, H. Nakatsuji, M. Hada, M. Ehara, K. Toyota, R. Fukuda, J. Hasegawa, M. Ishida, T. Nakajima, Y. Honda, O. Kitao, H. Nakai, M. Klene, X. Li, J. E. Knox, H. P. Hratchian, J. B. Cross, V. Bakken, C. Adamo, J. Jaramillo, R. Gomperts, R. E. Stratmann, O. Yazyev, A. J. Austin, R. Cammi, C. Pomelli, J. W. Ochterski, P. Y. Ayala, K. Morokuma, G. A. Voth, P. Salvador, J. J. Dannenberg, V. G. Zakrzewski, S. Dapprich, A. D. Daniels, M. C. Strain, O. Farkas, D. K. Malick, A. D. Rabuck, K. Raghavachari, J. B. Foresman, J. V. Ortiz, Q. Cui, A. G. Baboul, S. Clifford, J. Cioslowski, B. B. Stefanov, G. Liu, A. Liashenko, P. Piskorz, I. Komaromi, R. L. Martin, D. J. Fox, T. Keith, M. A. Al-Laham, C. Y. Peng, A. Nanayakkara, M. Challacombe, P. M. W. Gill, B. Johnson, W. Chen, M. W. Wong, C. Gonzalez and J. A. Pople, *Gaussian 09*, revision A.2, Gaussian, Inc., Wallingford, CT, 2009.
- S4. SAINT+, ver. 6.02a, Bruker Analytical X-ray System, Inc., Madison, WI, **1998**.
- S5. G. M. Sheldrick, SADABS, Empirical Absorption Correction Program, University of Göttingen, Germany, **1997**.

S6. G. M. Sheldrick, SHELXTLTM, Reference Manual, ver. 5.1, Madison, WI, **1997**.

Structural discussion

Coordination configuration of Ir-SO₂O: The coordination arrangement around the Ir^{III} center of **Ir-SO₂O** consists of a distorted octahedral geometry with the bond angles C(24)-Ir(1)-O(5) of 173.0(6) $^{\circ}$, C(11)-Ir(1)-O(4) of 173.4(6) $^{\circ}$ and N(1)-Ir(1)-N(2) of 175.4(6) $^{\circ}$. The bond angles C(11)-Ir(1)-C(24) of 95.2(7) $^{\circ}$, O(4)-Ir(1)-O(5) of 88.5(5) $^{\circ}$ and N(1)-Ir(1)-N(2) of 175.4(6) $^{\circ}$ indicate the *cis*-O,O, *cis*-C,C, and *trans*-N,N chelate disposition around the Ir^{III} center.

Table S1 Crystal data for **Ir-SO₂O**.

Compound	Ir-SO₂O
Formula	C ₃₉ H ₃₁ IrN ₂ O ₅ S
Formula weight	831.92
Crystal size (mm)	0.30 × 0.26 × 0.24
Crystal system	Triclinic
Space group	P-1
<i>a</i> (Å)	9.669(2)
<i>b</i> (Å)	12.029(3)
<i>c</i> (Å)	14.928(4)
α (°)	81.042(4)
β (°)	89.413(5)
γ (°)	89.088(4)
<i>V</i> (Å ³)	1714.8(7)
<i>Z</i>	2
<i>D</i> _{calc} (g cm ⁻³)	1.611
μ (mm ⁻¹)	4.001
<i>F</i> (0 0 0)	824
<i>T</i> (K)	293
2θ Range (°)	1.38 – 24.00
Number of reflections collected	7959
Number of unique reflections	5343
<i>R</i> _{int}	0.0724
Number of reflections with <i>I</i> >2.0σ(<i>I</i>)	2945
Number of parameters	362
<i>R</i> _{1,wR₂} [<i>I</i> >2.0σ(<i>I</i>)] ^a	0.0777, 0.1436
<i>R</i> _{1,wR₂} (all data)	0.1770, 0.2355
GoF on <i>F</i> ² ^b	0.957

^a $R_1 = \sum ||F_o| - |F_c|| / \sum |F_o|$. $wR_2 = \{ \sum [w(F_o^2 - F_c^2)^2] / \sum [w(F_o^2)^2] \}^{1/2}$.

^b GoF = [($\sum w|F_o| - |F_c|$)² / ($N_{\text{obs}} - N_{\text{param}}$)]^{1/2}.

Table S2 Photophysical, electrochemical and thermal data for **Ir-SO₂O** and **Ir-SO₂N**

	Absorption (293K) ^a λ_{abs} (nm)	Emission (293K) λ_{em} (nm)	Φ_p ^b	τ_p ^c 293 K/77 K (μs)	τ_r ^d (μs)	$\Delta T_{5\%}/T_g$ (°C)
Ir-SO₂O	268 (4.62), 284 (4.63), 358 (3.86), 397 (3.65), 430 (3.47), 490 (3.17), 520 (2.60)	556	0.52	0.99/4.85	1.90	344/153
Ir-SO₂N	259 (4.67), 284 (4.66), 359 (4.31), 388 (4.31), 436 (3.93), 497 (3.22), 523 (2.82)	564	0.35	0.81/4.95	2.31	334/153

^a Measured in CH₂Cl₂ at a concentration of 10⁻⁵ M, and log ε values are shown in parentheses. ^b In degassed CH₂Cl₂ relative to *fac*-[Ir(ppy)₃] ($\Phi_p = 0.40$), $\lambda_{\text{ex}} = 360$ nm. ^c Measured in degassed CH₂Cl₂ solutions at a concentration of *ca.* 10⁻⁵ M, and the excitation wavelength was set at 370 nm for all the samples at 293 K. ^d The triplet radiative lifetimes (τ_r) were deduced from $\tau_r = \tau_p/\Phi_p$.

Table S3 The contribution of metal d_{π} orbital to the HOMO and LUMO levels together with the TD-DFT calculation results.

Compound	Contribution of metal d_{π} orbitals to HOMO	Contribution of metal d_{π} orbitals to LUMO	The largest coefficient in the CI expansion of the T_1 state ($S_0 \rightarrow T_1$ excitation energy) ^a	The largest coefficient in the CI expansion of the S_1 state ($S_0 \rightarrow S_1$ excitation energy) ^a	The oscillator strength (f) of the $S_0 \rightarrow S_1$ transition
Ir-SO₂O	40.77%	3.41%	H→L: 0.65298 (518.7 nm)	H→L: 0.68708 (465.9 nm)	0.0210
Ir-SO₂N	4.74%	3.41%	H→L: 0.51536 (522.9 nm)	H→L: 0.63732 (477.4 nm)	0.0121

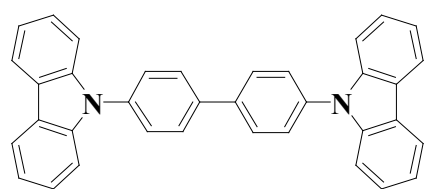
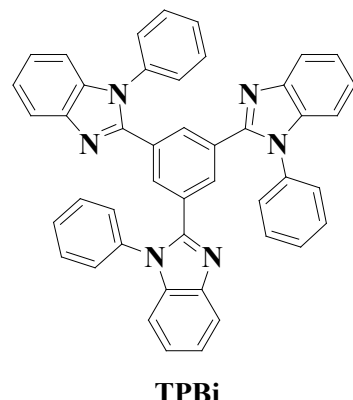
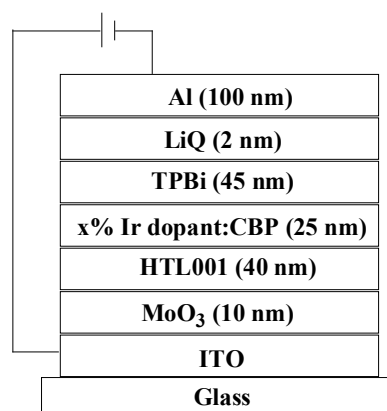
^a H→L represents the HOMO to LUMO transition. CI stands for configuration interaction.

Table S4 Redox properties of Ir-SO₂O and Ir-SO₂N

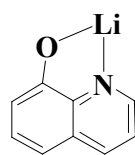
Complex	$E_{1/2}^{\text{ox}}$ (V)	$E_{1/2}^{\text{red}}$ (V)	HOMO (eV)	LUMO (eV)
Ir-SO₂O	0.44, 0.49	-2.30, -2.63	-5.24	-2.50
Ir-SO₂N	0.34, 0.46	-2.31, -2.66	-5.14	-2.49

Table S5 The hole/electron reorganization energy (λ_h/λ_e) for **Ir-SO₂O** and **Ir-SO₂N** calculated by the DFT method

Complex	λ_h (eV)	λ_e (eV)	$\lambda_e - \lambda_h$ (eV)
Ir-SO₂O	0.28	0.41	0.13
Ir-SO₂N	0.16	0.39	0.23



CBP



LiQ

Dopant Devices and doping level

Ir-SO₂O **A1** (3 wt.-%), **A2** (6 wt.-%), **A3** (8 wt.-%), **A4** (9 wt.-%), **A5** (10 wt.-%), **A6** (12 wt.-%)

Ir-SO₂N **B1** (6 wt.-%), **B2** (9 wt.-%), **B3** (12 wt.-%), **B4** (15 wt.-%)

Fig. S2 Device structure, chemical structures of the key compounds employed for the phosphorescent OLEDs prepared by **Ir-SO₂O** and **Ir-SO₂N**.

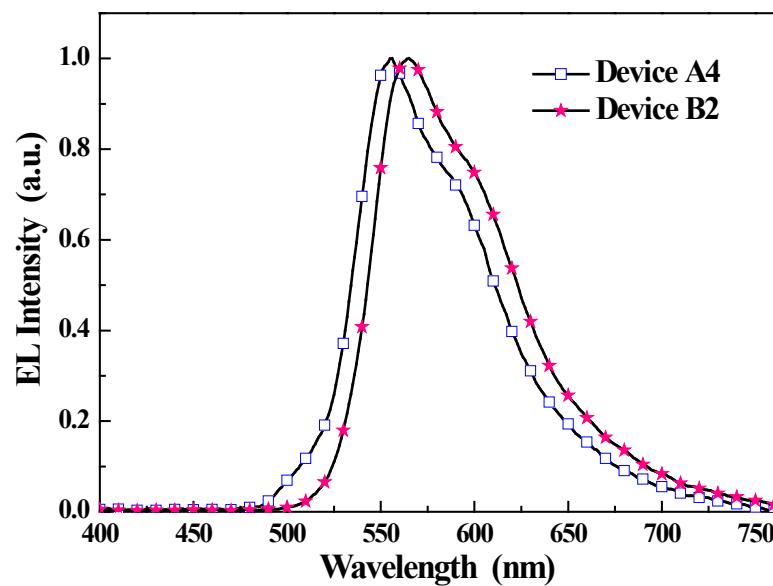


Fig. S3 The EL spectra for the devices **A4** and **B2** at *ca.* 8V.

Table S6 The maximum EL performance of the asymmetric Ir^{III} complexes and their symmetric analogues in doped phosphorescent OLEDs under the same experimental conditions.

Device	Phosphor dopant	L_{\max}^{a} (cd m ⁻²)	$\eta_{\text{ext}}^{\text{a}}$ (%)	$\eta_{\text{L}}^{\text{a}}$ (cd A ⁻¹)	$\eta_{\text{p}}^{\text{a}}$ (lm W ⁻¹)	$\lambda_{\max}^{\text{b}}$ (nm)
A1	Ir-SO₂O (3 wt.-%)	17862 (14.0)	13.7 (7.2)	44.8 (7.2)	19.6 (7.2)	550 (0.41, 0.54)
A2	Ir-SO₂O (6 wt.-%)	22225 (14.0)	14.5 (7.2)	49.5 (7.2)	21.6 (7.2)	555 (0.44, 0.53)
A3	Ir-SO₂O (8 wt.-%)	52813 (14.0)	16.8 (6.2)	55.8 (6.2)	28.3 (6.2)	553 (0.43, 0.53)
A4	Ir-SO₂O (9 wt.-%)	43522 (14.0)	20.2 (6.2)	69.4 (6.2)	35.2 (6.2)	556 (0.45, 0.52)
A5	Ir-SO₂O (10 wt.-%)	69545 (14.0)	15.2 (5.6)	52.0 (5.6)	29.2 (5.6)	556 (0.46, 0.52)
A6	Ir-SO₂O (12 wt.-%)	43919 (14.0)	14.2 (6.0)	49.1 (6.0)	25.7 (6.0)	557 (0.47, 0.51)
B1	Ir-SO₂N (6 wt.-%)	48759 (14.0)	11.5 (7.2)	39.0 (7.2)	17.0 (7.2)	564 (0.49, 0.50)
B2	Ir-SO₂N (9 wt.-%)	50436 (14.0)	11.0 (7.2)	41.2 (7.6)	17.3 (7.4)	565 (0.50, 0.49)
B3	Ir-SO₂N (12 wt.-%)	55435 (14.0)	9.1 (8.4)	30.5 (8.4)	12.5 (7.6)	565 (0.50, 0.49)
B4	Ir-SO₂N (15 wt.-%)	66186 (14.0)	11.1 (5.4)	37.0 (5.4)	22.2 (5.2)	567 (0.50, 0.49)
C1	Ir-N (6 wt.-%)	47253 (14.0)	10.0 (6.2)	35.6 (6.2)	23.9 (5.8)	529 (0.35, 0.58)
C2	Ir-O (10 wt.-%)	46938 (14.0)	10.3 (6.2)	33.5 (6.2)	21.8 (6.2)	505 (0.26, 0.59)
C3	Ir-SO₂ (9 wt.-%)	47698 (14.0)	10.2 (6.4)	33.4 (6.4)	20.6 (6.2)	548 (0.43, 0.54)

^a The voltage at which the data were collected is shown in parentheses. ^b The CIE coordinates are shown in parentheses.

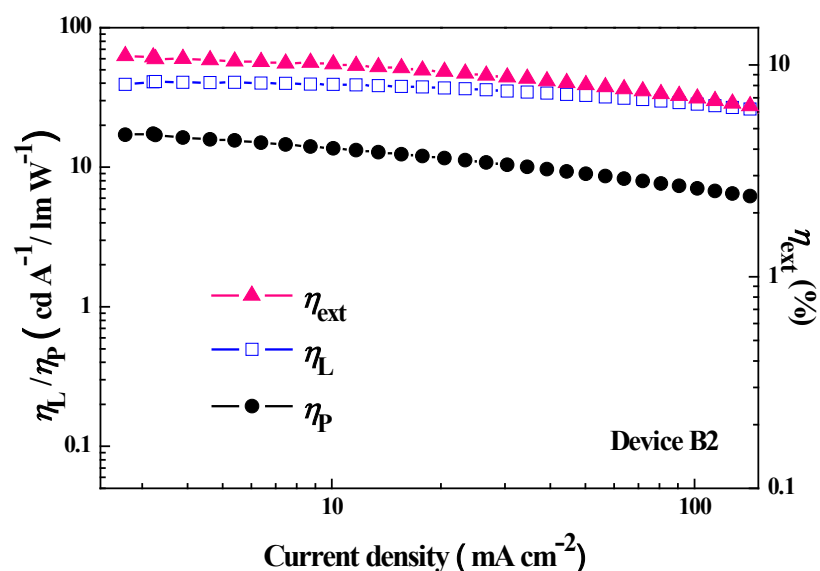


Fig. S4 The dependence relationship between EL efficiencies and current density for device **B2**.

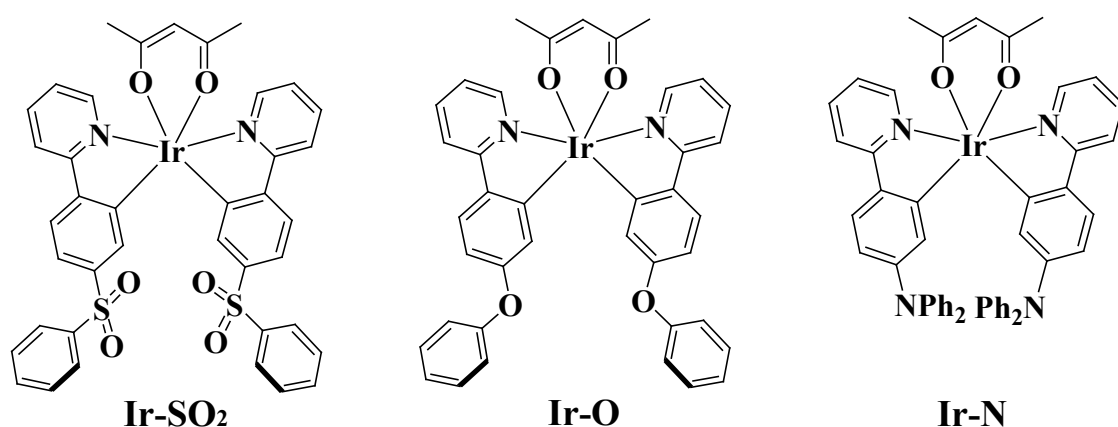


Fig. S5 The chemical structures of the symmetric heteroleptic Ir^{III} complexes **Ir-SO₂**, **Ir-O** and **Ir-N**.

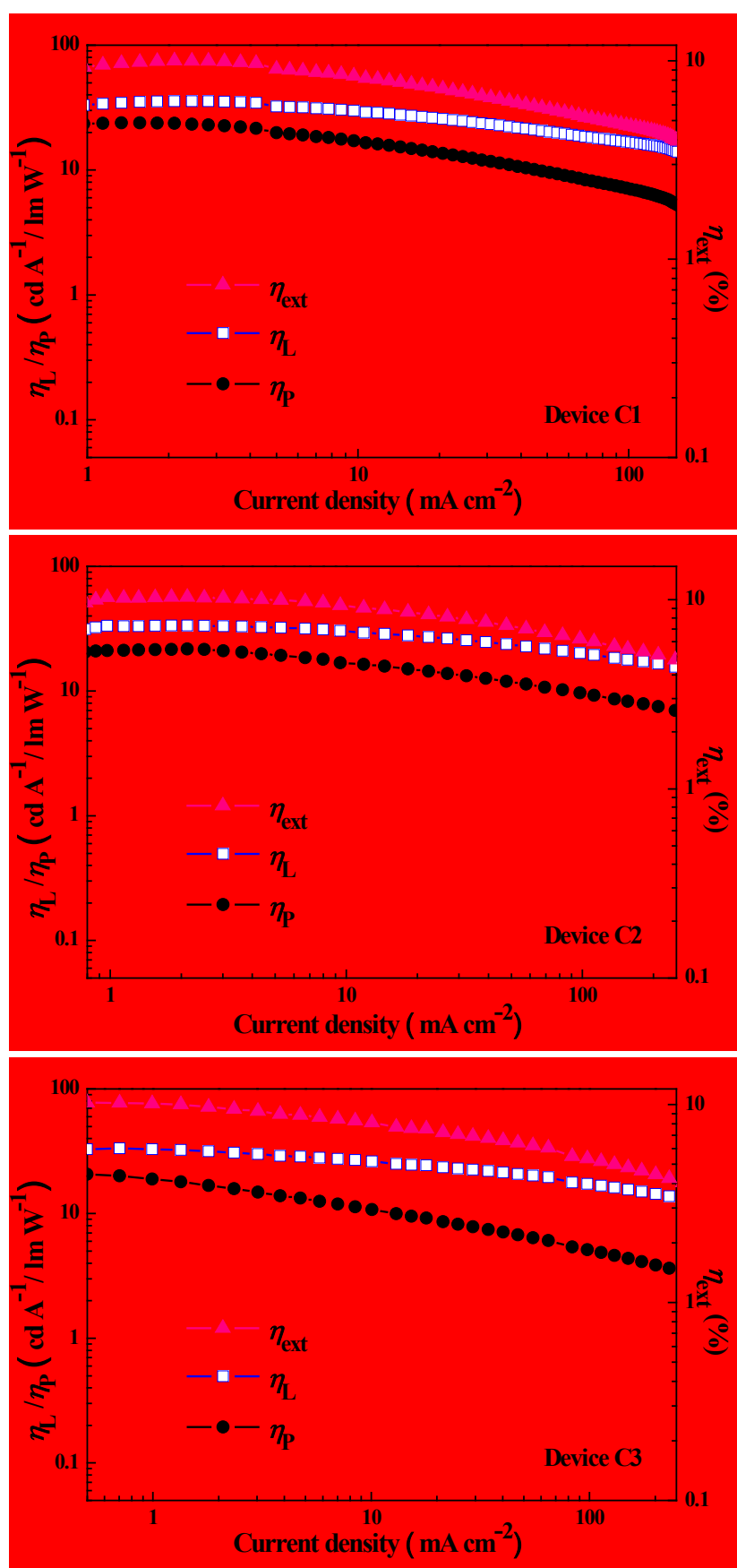
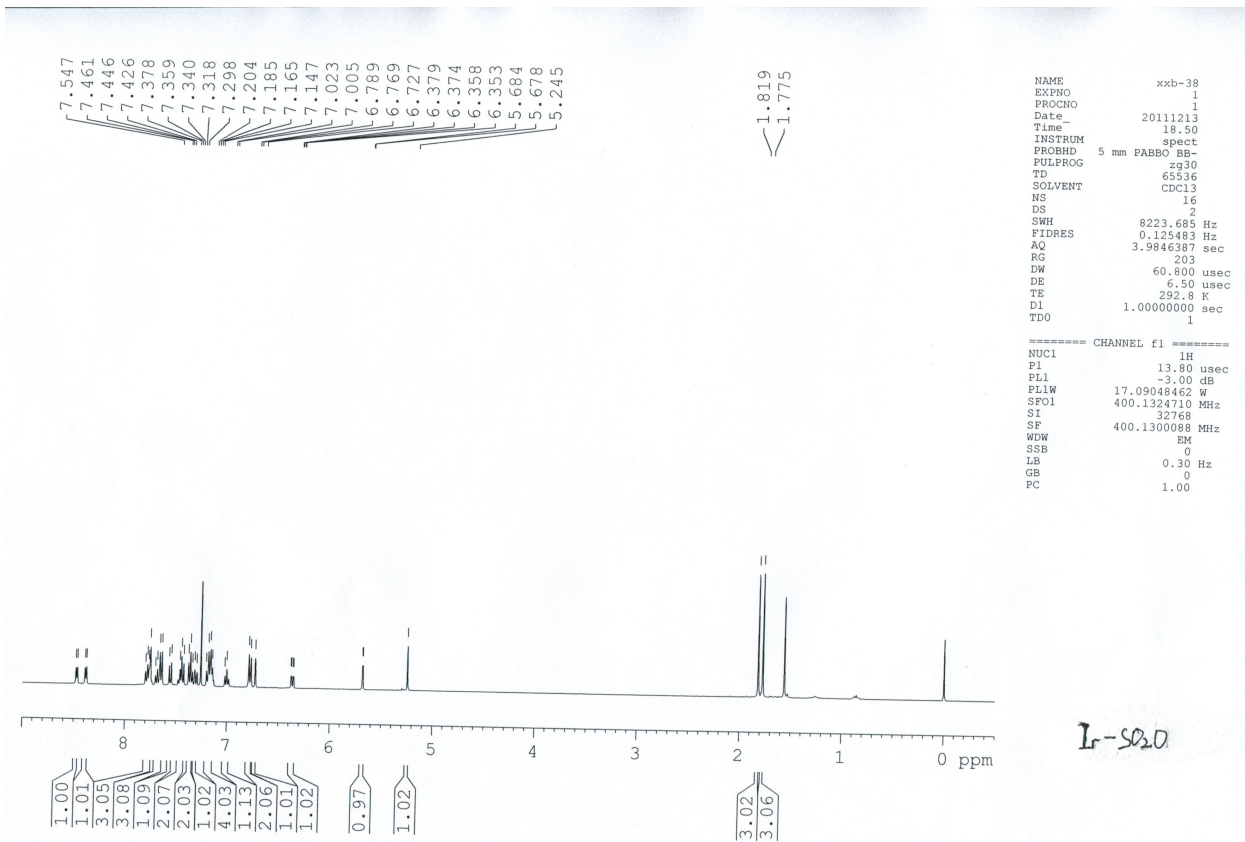
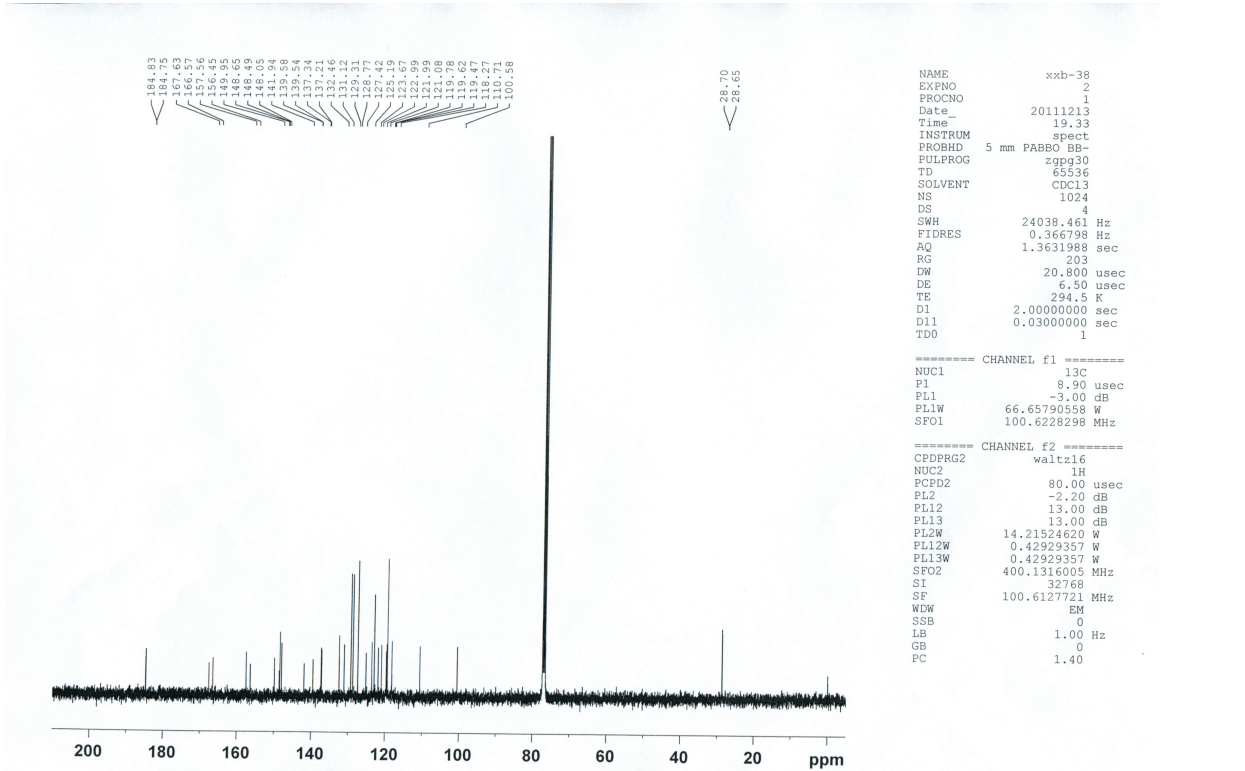


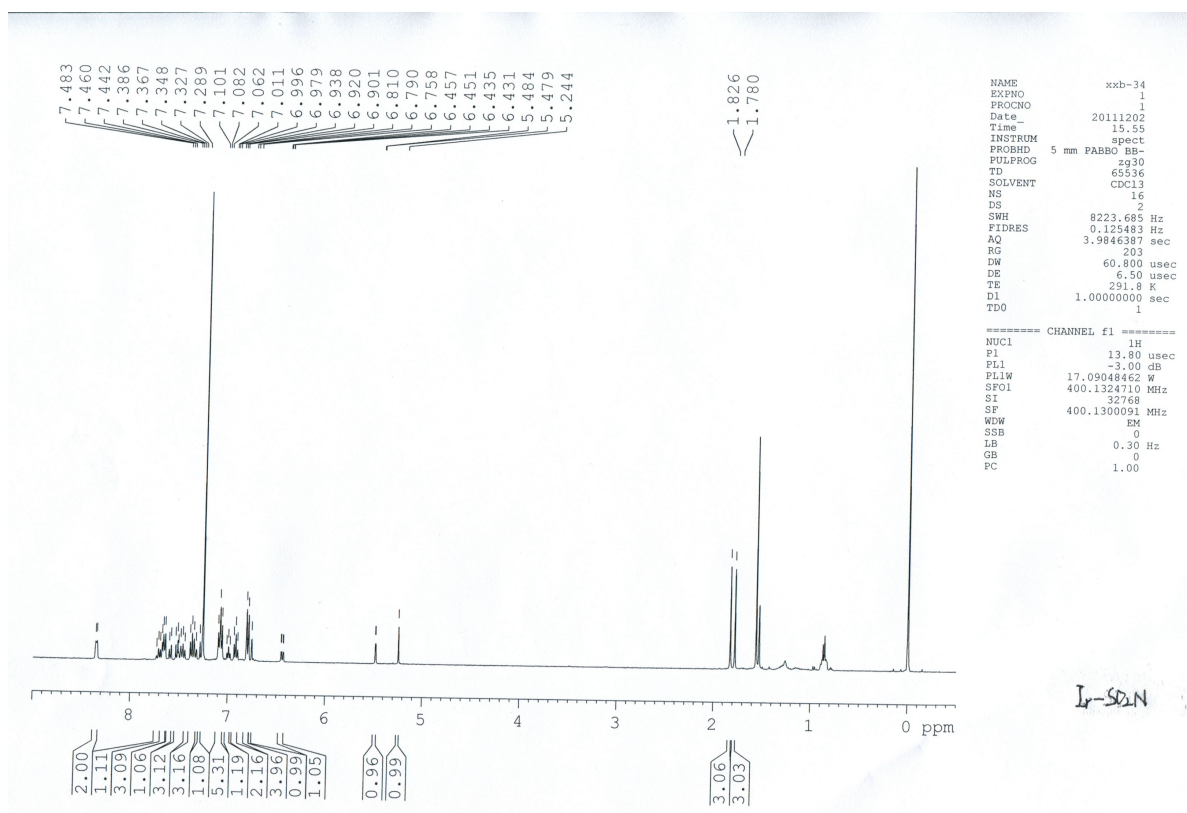
Fig. S6 The dependence relationship between EL efficiencies and current density for optimized devices made from the symmetric Ir^{III} complexes **Ir-N** (Device C1), **Ir-O** (Device C2), and **Ir-SO₂** (Device C3).



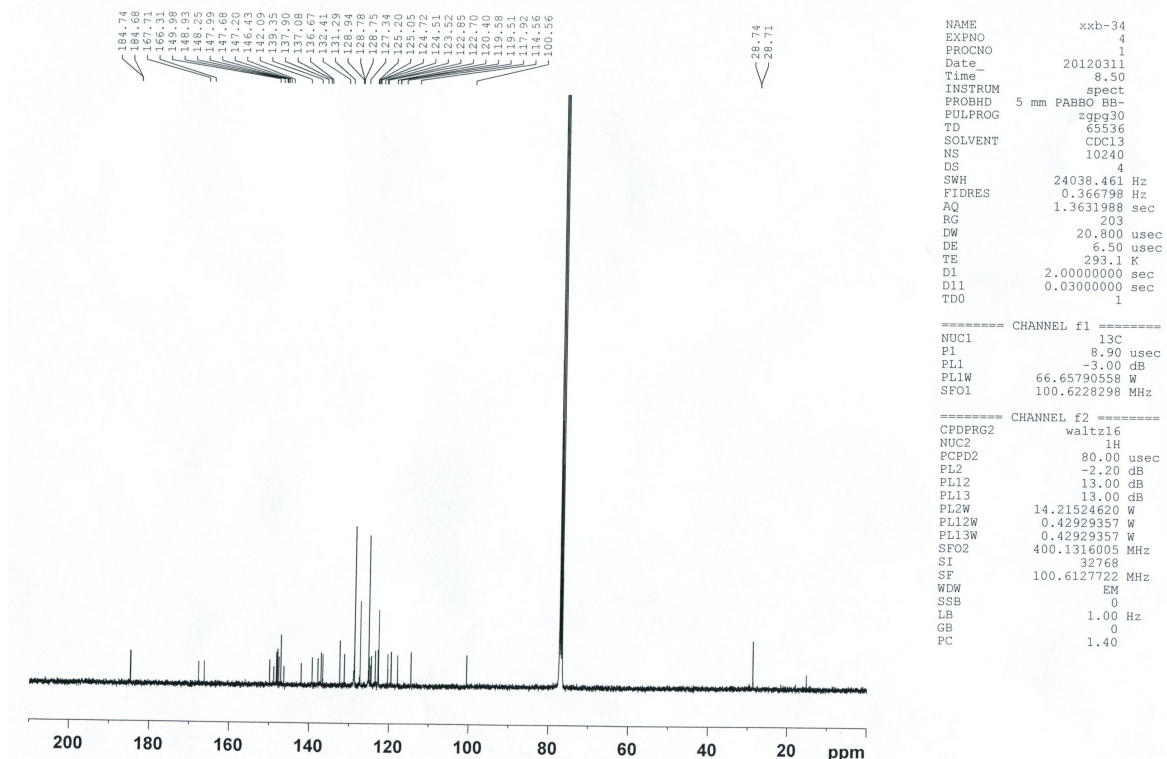
(a) ^1H -NMR spectrum for Ir-SO₂O



(b) ^{13}C -NMR spectrum for Ir-SO₂O



(c) ¹H-NMR spectrum for Ir-SO₂N



(d) ¹³C-NMR spectrum for Ir-SO₂N

Fig. S7 The NMR spectra for Ir-SO₂O and Ir-SO₂N.

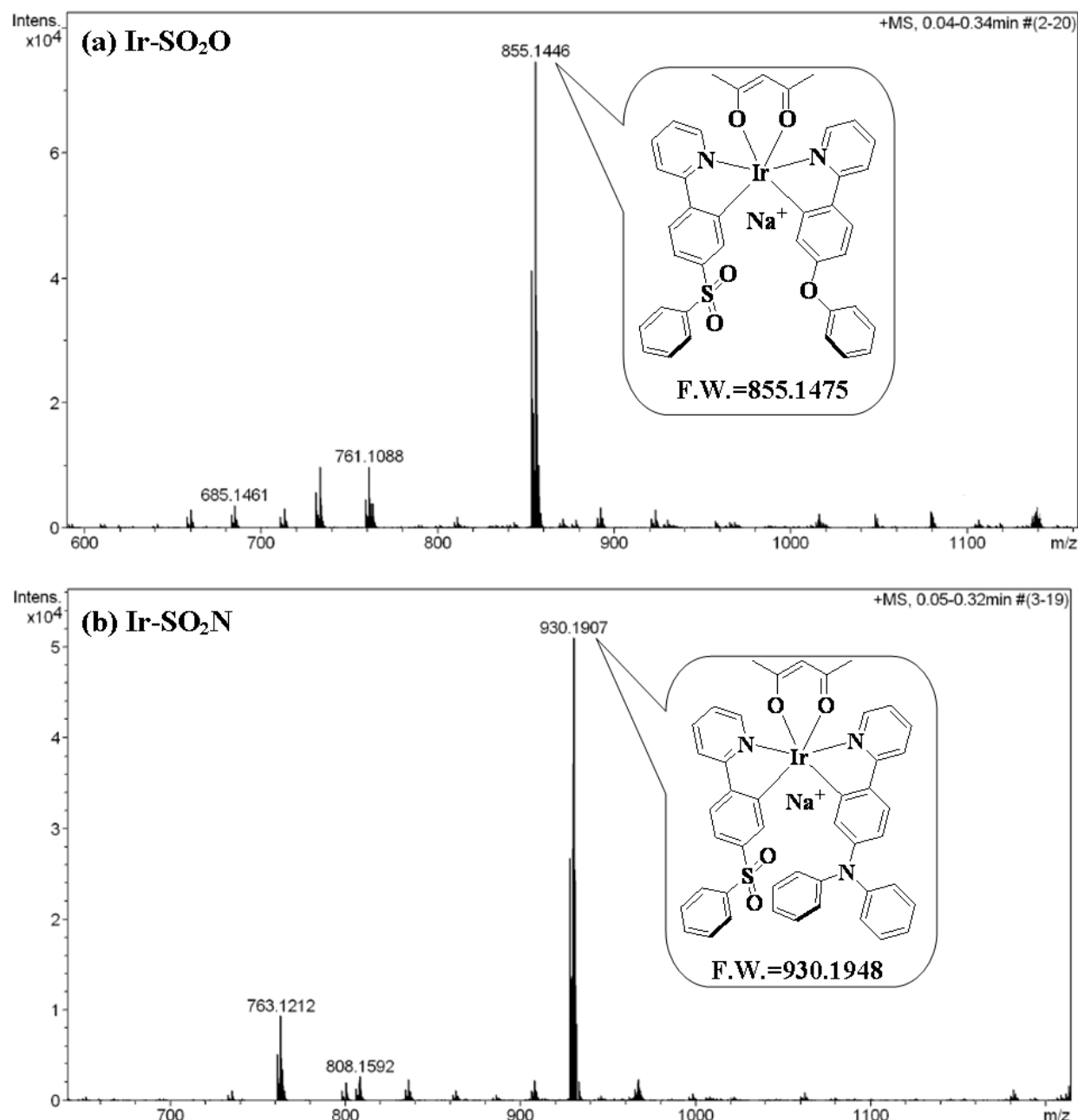


Fig. S8 The ESI-TOF mass spectra for Ir-SO₂O and Ir-SO₂N.